THE IMPACTS OF SMOKE AEROSOLS ON SOUTH AMERICAN MONSOON

Yongqiang Liu
USDA Forest Service/Forestry Sciences Laboratory, Athens, GA, USA
Rong Fu and Robert Dickinson
Georgia Institute of Technology, Atlanta, GA, USA

1. INTRODUCTION

Biomass burning has been extensively used in the past two decades to clean forest and savanna for agriculture use in tropical South America. Smoke aerosols released from biomass burning in this region can affect regional and global radiation through scattering and absorbing solar radiation (Penner et al.1992, Hobbs et al. 1997, Ross et al. 1998). This can further lead to perturbations in regional circulation, clouds and precipitation, and the land-surface processes (Koren et al. 2004, Andreae et al. 2004, Liu 2004).

The circulation and cloud perturbations could be a factor for the development of monsoon in South America, which usually starts shortly after a smoke season. The cloud and rainfall reduction could modify soil moisture, which has the capacity to retain anomalous signals in the land-atmosphere system at monthly to seasonal scales (Vinnikov et al. 1996). Thus, perturbations in the land-atmosphere system caused by biomass burning can last for a period of time beyond a smoke season and, therefore, affect the monsoon process.

This study seeks to understand the effects of biomass burning on the South American monsoon by investigating the case of smoke season and monsoon development during 1995. It extends a recent effort (Liu 2004) in simulating the direct radiative and climatic effects of biomass burning with the NCAR regional climate model (RegCM) (Dickinson et al. 1989, Giorgi and Bates 1989).

2. SIMULATION SETUP

The simulation setup is similar to that in Liu (2004). Thus, only a brief description is given here. The simulation domain (Fig.1) covers most of South America with 91×91 grid points and 14 vertical layers up to 80 hPa. The resolution is 60 km. The initial and horizontal lateral boundary conditions of wind, temperature, water vapor, and surface pressure are interpolated from the analysis of the European Center for Medium Range Weather Forecast (ECMWF). Soil water content is initialized depending on type of vegetation (Giorgi and Bates 1989).

•*Corresponding author address*: Yongqiang Liu, Forest Sciences Laboratory, 320 Green Street, Athens, GA 30602; e-mail: yliu@fs.fed.us

A control simulation without smoke loading and a smoke simulation with smoke loading were conducted for the smoke phase (August and September) of 1995 (Liu 2004). In the smoke simulation, the smoke optical properties, including total optical depth (TOD), single scattering albedo (SSA) and asymmetric factor, were specified based on the SCAR-B measurements (Kaufman et al. 1998). The midvisible optical depth of 0.75 were adopted (Ross et al. 1998) for the smoke region. The land areas other than the smoke region and the Andes Mountains were assumed to have a background optical depth of 0.12. An SSA of 0.88 was specified for the smoke approximately at 0.55 μm based on the measured range of 0.82 for young smoke and 0.94 for aged smoke (Eck et al. 1998). Wavelength dependencies of the optical properties were determined mainly based on the fourth-order polynomials (Ross et al. 1998). Humidification effect has been included in the optical depth. Smoke particles were assumed to be retained within the smoke region and to be evenly distributed in a layer between the ground and about 2.5 km throughout the simulation period.

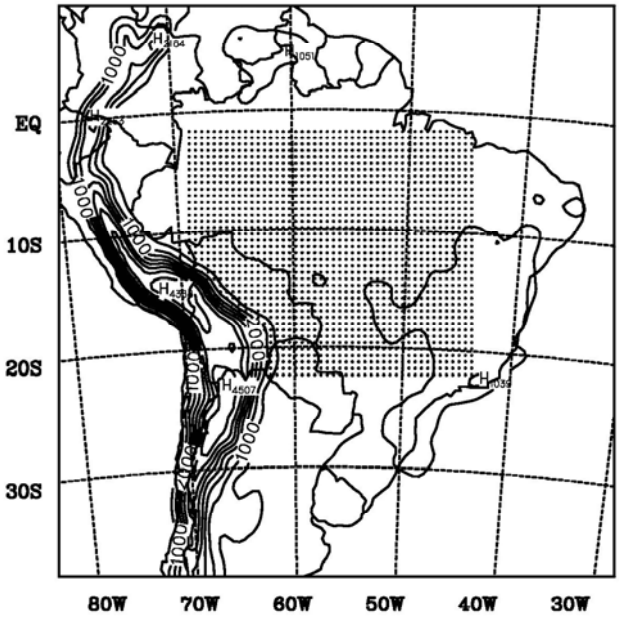

Fig. 1. The simulation domain with the biomass burning region shaded by dots. The interval of topography is 500 m (after Liu 2004).

In the present study, the two simulations described above are continuously run for the monsoon phase (October and November). There is no more smoke loading in the smoke simulation during this phase. The effects of biomass burning are measured by the differences in the simulated circulation, precipitation, and the land-surface processes during the monsoon phase between the smoke and control simulations.

3. RESULTS

3.1 Circulations

The planetary-scale Atlantic high pressure system is dominant over the biomass burning region during the first month of the smoke phase (Fig.2a). The area with the geopotential height greater than 5860 extends across the continental. In the mid-latitudes is the westerly trough system and over the Caribbean Sea coast is a tropical trough system. The high pressure system becomes weaker and withdraws eastwards in the second month of the smoke phase (Fig.2b). During the monsoon phase (Fig.2c-d), this system moves further east and disappears from the simulation domain.

The perturbation in the 500 hPa geopotential height induced by smoke aerosols is mostly positive during the smoke phase (Fig.2e-f), indicating that the high pressure system becomes more intensive due to biomass burning. The magnitude is larger in the second month than in the first one with the most significant perturbation found in the northwestern section of the biomass burning region. The positive perturbation exists even after biomass burning has ceased (Fig.2g). The sign of the perturbation during the first month of the monsoon phase is the same as the smoke phase, but the magnitude is smaller and the location moves southward.

The monsoon progress is tracked by following the eastward withdrawal of the Atlantic high pressure system. Fig.3 shows longitude-time cross-section of the 500 hPa geopotential height averaged over the grid points 30-60 in the south-north direction. This system is assumed to be bounded by the geopotential height of 5860 m (the shaded areas in Fig.3a). The system extends westward to about 70^{o}W in the first a few days into simulation (i.e., early August). It further extends beyond 80^{o}W about 20 days into simulation and stays there for about 20 days. Then it withdraws rapidly to about 55^{o}W and stays there for about one month until moving out of the eastern boundary of the simulation domain in early October. The disappearance happens a few days after the termination of biomass burning in the model.

The systematic positive perturbation in the 500 hPa geopotential height (Fig.3b) appears about 10 days into simulation. The largest magnitude is found in the first half of the second month (September) of the smoke phase. The perturbation is visible about 10 days after the termination of biomass burning.

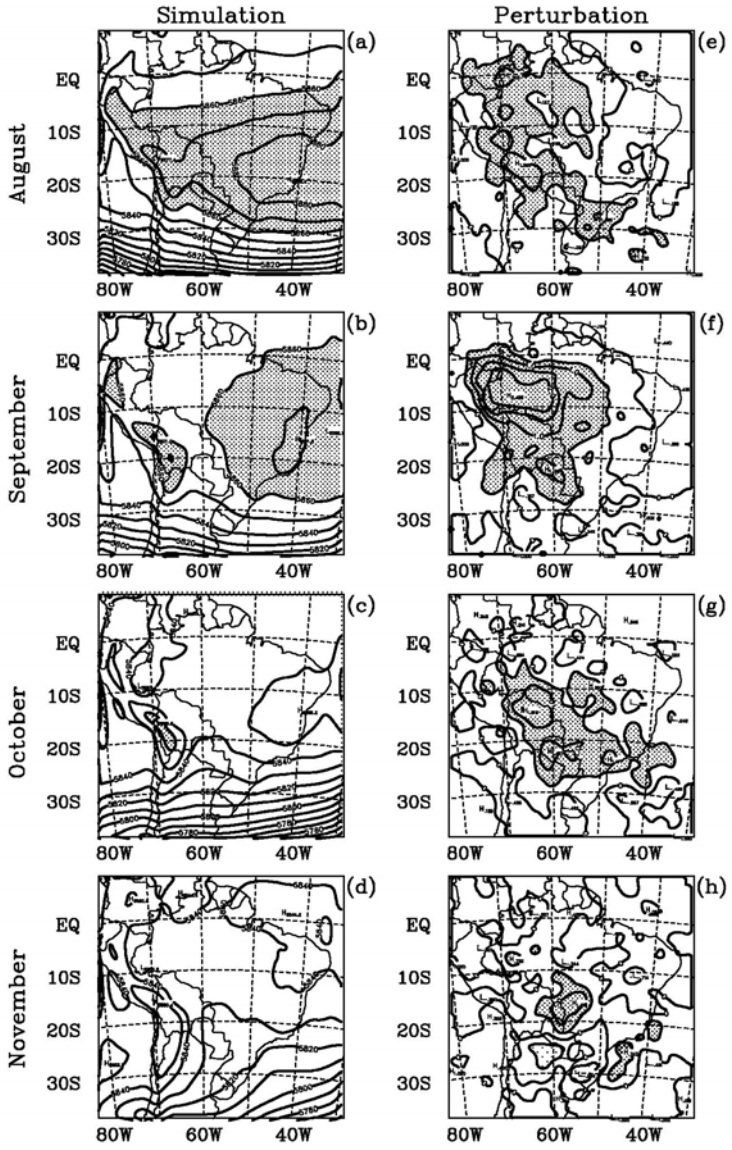

Fig. 2 The 500 hPa geopotential height (m) from August to November (from top to bottom). The left panels are the control simulation. The contour interval is 10 m with the values greater than 5860 m shaded. The right panels are the difference between the smoke and control simulations. The contour interval is 0.5 m with the values greater than 0.5 m and less than -0.5 m shaded with dense and coarse dots, respectively.

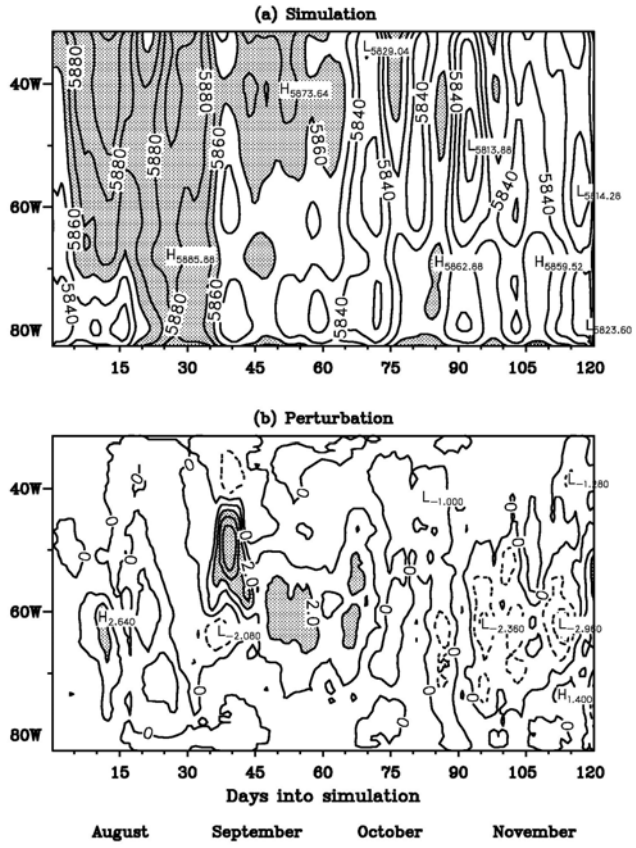

Fig.3 Longitude-time cross-section of the 500 hPa geopotential height (m) averaged over the grid points 30-60 in south-north direction. The top is the control simulation. The contour interval is 10 m with the values greater than 5860 m shaded. The bottom is the difference between the smoke and control simulations. The contour interval is 1m with the values greater than 2 m and less than -2 m shaded with dense and coarse dots, respectively.

3.2 Precipitation

The simulated rainfall rate is about 2 mm/day in the beginning (Fig.4a). It reduces to nearly none within 10 days and remains very small in the following month. Then it increases with time and reaches the level of 2~2.5 mm/day by 65 days into simulation. There is a large precipitation event in the next 10 days during which rainfall jumps to about 6~7.5 mm/day. Rainfall is around 4 mm/day in the following month and then jumps again in the end of the simulation period.

The biomass burning has little effects on rainfall in August, during which period rainfall itself is very small. Negative perturbation in rainfall appears in early September with the largest amount of about -1 and -0.5 mm/day over the biomass burning region and entire continental, respectively. The sign remains negative until about 75 days into simulation, and fluctuates over time thereafter.

3.3 Land-Surface Processes

Evolution of the simulated land-surface hydrological properties, including the surface-layer soil moisture (Fig.4b) and evapotranspiration (Fig.4c), closely follow that of rainfall. So does their perturbation induced by smoke aerosols. Similar to rainfall, the perturbation in either property lasts for about half a month after the termination of biomass burning. One difference from rainfall perturbation is that the surface-layer soil moisture perturbation has a large positive value and remains positive during entire August. This is related to the large reduction in evapotranspiration, which in turn results from the ground cooling (to be shown shortly). The perturbation in the root-layer soil moisture (not shown) has a similar trend in temporal variation to that in the surface-layer soil moisture except that the positive sign remains during the entire simulation period.

The simulated ground temperature (Fig.4d) and sensible heat flux (Fig.4e) increase gradually with time during August and then remain less varied during September. They turn to lower during the monsoon phase in response to the increased rainfall. The scattering and absorption by smoke aerosols prevent part of solar radiation from reaching the ground, leading to cooling on the ground. The ground temperature is reduced during the smoke phase by about 3 and 1.5^{o}C over the biomass burning region and the entire continental, respectively. Sensible heat flux is reduced by about 50 and 25 Wm^{-2}, respectively. The perturbations in temperature and sensible heat flux, which are mainly land-surface thermal properties, however, disappear much faster than those of rainfall and the land-surface hydrological properties after the termination of biomass burning.

3.4 Mechanisms

It is shown above that the effects of biomass burning during the smoke phase can last for about half a month into the monsoon phase. Studies have indicated the important property of soil moisture in retaining anomalous signals over long periods (e.g., Delworth and Manabe 1989, Vinnikov et al. 1996, Liu and Avissar 1999). As a result, soil moisture can contribute to long-term atmospheric variability over land by passing its relatively slow anomalous signals to the atmosphere. To analyze the possible role of soil moisture in the effects of biomass burning on the subsequent monsoon, two experiment simulations (control-soil and smoke-soil) are performed. They are the same as the control and smoke simulations except that soil moisture values of the three model layers are fixed during the integration.

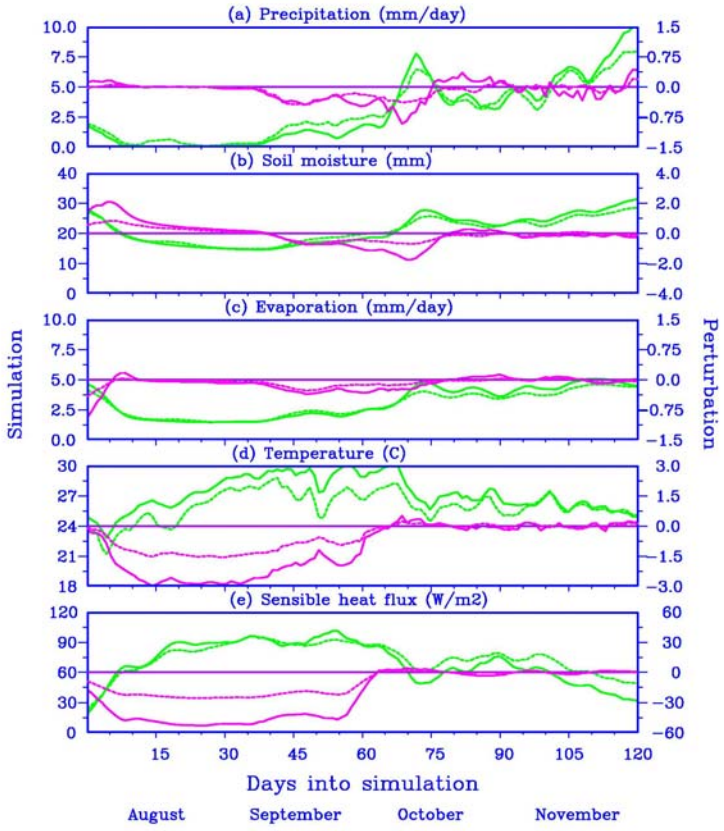

Fig.4 Temporal variations of the land-surface variables and fluxes. The green and red lines represent the control simulation and the difference between the smoke and control simulations, respectively. The solid and dashed lines represent the averages over the biomass burning region and the entire continental, respectively.

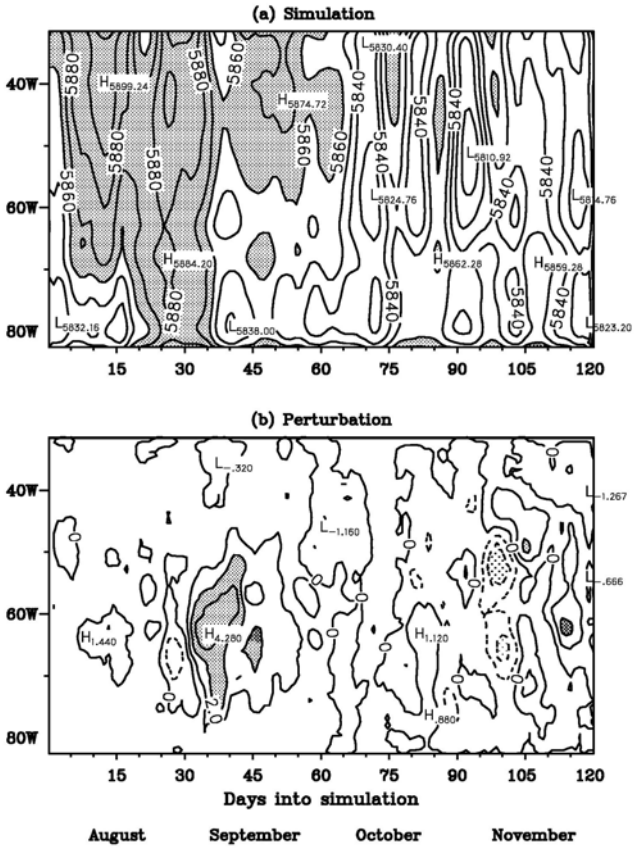

Fig.5 Same as Fig.3 except for the simulations with fixed soil moisture.

In comparison with the control simulation, the control-soil simulation produces a much larger evapotranspiration (Fig.6c), which is mostly caused by larger soil water availability. This leads to a lower ground temperature (Fig.6d) and lower sensible heat flux (Fig.6e).

Without the interactions between soil moisture and the atmospheric processes, the systematic positive perturbation (i.e., the difference between the smoke-soil and control-soil simulations) in the 500 hPa geopotential height averaged over the grid points 30-60 does not last beyond the smoke phase (Fig.5b). No significant perturbation in rainfall is found during both the smoke and monsoon phases (Fig.6a). Perturbation in evapotranspiration becomes more significant during the smoke phase, but it disappears right after the termination of biomass burning. These results suggest that soil moisture variability should be one of the mechanisms for the effects of biomass burning on the monsoon process.

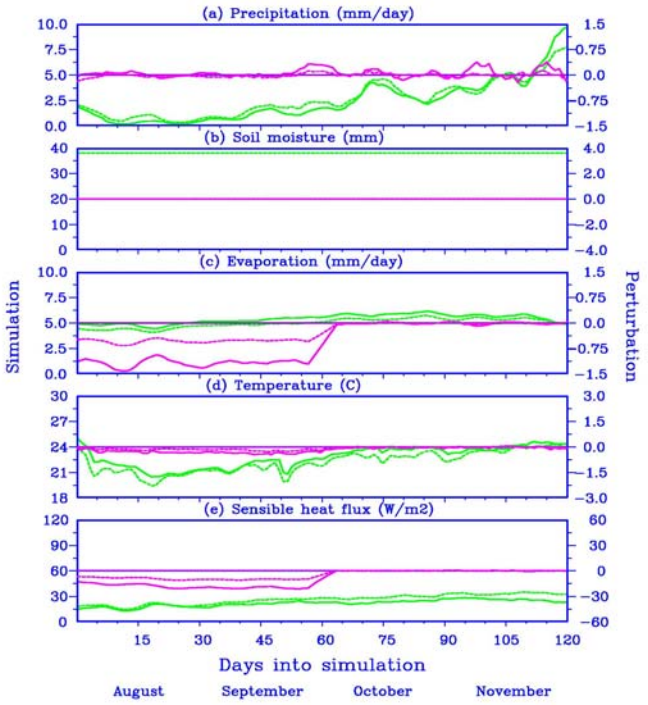

Fig.6 Same as Fig.4 except for the simulations with fixed soil moisture.

4. SUMMARY

Simulations with the NCAR regional climate model have been conducted to examine the effects of biomass burning on the South American monsoon for the 1995 smoke season. The results have shown that the Atlantic high becomes more intensive due to biomass burning during the smoke phase. This perturbation is also seen in the first month of the subsequent monsoon phase, indicating that biomass burning could affect adversely the development of the summer monsoon. The hydrological interactions between soil and the atmosphere could be one of the mechanisms for the effects of biomass burning on the monsoon process.

Acknowledgement This study was supported by the USDA Forest Service National Fire Plan through the Southern High-Resolution Modeling Consortium (SHRMC) and by the U.S. National Science Foundation (Award 0203761).

References

Andreae, M.O., D. Rosenfeld, P. Artaxo, A.A. Costa, G.P. Frank, K.M. Longo, and M.A.F. Silva-Dias, 2004, Smoking rain clouds over the Amazon, *Science*, **303**, 1337-1342.

Delworth T. and S. Manabe, 1989, The influence of soil wetness on near-surface atmospheric variability. *J. Clim*., **2**, 1447-1462.

Dickinson, R. E., R. M. Errico, F. Giorgi, and G. T., Bates, 1989, A regional climate model for the western U.S., *J. Clim.,* **15**, 383-422.

Eck, T.F., B.N. Holben, I. Slutsker, and A. Setzer, 1998, Measurements of irradiarance attenuation and estimation of aerosol single scattering albedo for biomass burning aerosols in Amazonia, *J. Geophys. Res*., **103**, 31865-31878.

Giorgi, F. and G. T. Bates, 1989, The climatological skill of a regional model over complex terrain, *Mon. Wea. Rev*., **117**, 2325-2347.

Hobbs, P.V., J.S. Reid, R.A. Kotchenruther, R.J. Ferek, and R. Weiss, 1997, Direct radiative forcing by smoke from biomass burning, *Science*, **275**, 1176-1178.

Kaufman Y.J., P.V. Hobbs, V.W.J.H. Kirchhoff, P. Artaxo, L.A. Remer, B.N. Holben, M.D. King, D.E. Ward, E.M. Prins, K.M. Longo, L.F. Mattos, C.A. Nobre, J.D. Spinhirne, Q. Ji, A.M. Thompson, J.F. Gleason, S.A., Christopher, and S.-C. Tsay, 1998, Smoke, Clouds, and Radiation-Brazil (SCAR-B) experiment, *J. Geophys. Res*., **103**, 31783-31808.

Koren, I, Y.J. Kaufman, L.A. Remer, and J.V. Martins, 2004, Measurement of the effects of Amazon smoke on inhibition of cloud formation, *Science*, **303**, 1342-1345.

Liu, Y.-Q., and R. Avissar, 1999, A study of persistence in the land-atmosphere system with a fourth-order analytical model, *J. Clim*., **12**, 2154-2168.

Liu, Y.-Q., 2004, Atmospheric response and feedback to radiative forcing from biomass burning in tropical South America, *Agri. Forestry. Meteor*. (Accepted).

Penner, J.E., R.E. Dickinson, and C.S. O'Neill, 1992, Effects of aerosol from biomass burning on the global radiation budget, *Science*, **256**, 1432-1434.

Ross J.L., P.V. Hobbs and B. Holben, 1998, Radiative characteristics of regional hazes dominated by smoke from biomass burning in Brazil: Closure tests and direct radiative forcing, *J. Geophys. Res*., **103**, 31925-31941.

Vinnikov, K., A. Robock, N.A. Speranskaya, and C.A. Schlosser, 1996, Scales of temporal and spatial variability of midlatitude soil moisture, *J. Geophys. Res*., **101**, 7163-7174.